Activated Carbon Pellets Prepared from KOH Treated Pre-Carbonized Palm Leaves (*Phoenix dactylifera* L.): Structures and Surface Functional Groups

Abubaker Elsheikh Abdelrahman[1]*, Fatima Musbah Abbas[2] and Abdul Kariem Arof[3]

[1]*Associate Professor, Director of Act center for Research, Singa, Sudan*

[2]*King Khalid University, Collage Science and Art, Dhahran Aljanoub, Abha, Saudi Arabia and Biotechnology and Genetic Engineering, National Center Researcher, Khartoum, Sudan*

[3]*Department of Physics, Centre for Ionics, University of Malaya, Kuala Lumpur, Malaysia*

Abstract

Series of activated carbon pellets were prepared from date palm leaves (*Phoenix dactylifera L.*) (DPL) primarily pre-carbonized at lower temperature and converted into fine grain powder to produce self-adhesive properties. The grain powder produced was chemically activated with KOH having a concentration of (0.0 - 0.09) by moles (M) converted into a pellet by applying 12 metric tons of pressure, before being carbonized at 1000ºC in a nitrogen environment, using a multi-step heating profile. Wide angle X-ray diffraction (XRD) was used to characterize the crystalline structure and estimate the crystallite parameters (d_{002}, L_c and L_a) and amorphous contents of the activated carbon produced. The surface function groups were analyzed by FTIR transmission spectra. X-ray diffraction analysis shows that the structure of the activated carbon produced is non-graphitic. The interlayer spacing (d_{002}) increased linearly with increasing KOH concentrations, while stack diameter (L_a) and stack height (L_c) of the graphitic like crystal were observed to decrease with increasing KOH concentrations. The amorphous contents were decreased for AC treated with 0.1 M and 0.2 M of 49% and 48% respectively and further increased from 0.02 M to 59% amorphous. The KOH treatment process, The FTIR transmission spectrum of the carbon pellets showed the presence of some bands related to organic compounds, which were still not completely released in the AC pellets. Implies that the surface organic functional groups occurring were due to the change in surface nature caused by the KOH treatment process.

Keywords: Activated carbon pellets • Date palm leaves • KOH • Crystallites parameters • Amorphous contents • Surface function groups

Introduction

Activated carbon is the collective name for a group of porous carbons manufactured to exhibit extraordinary application in different fields such a wastewater treatment and absorption [1-3] effective electromagnetic wave absorption [4] super capacitor [5] and double layer capacitor [6] due to unique pore structure, a high specific surface area and chemical stability. Very often, carbonizing carbonaceous carbon such as biomass and agricultural by-products, will produce carbon materials as the main product and different volatile compounds as by-product [7,8] Therefore, there are many carbonaceous material can be used to prepare activated carbon materials can be produced by either treatment of a char with oxidizing gases, or carbonization of carbonaceous materials with simultaneous activation by a chemical or physical process [8-12]. In a chemical activation process, the starting materials are first soaked with dehydrating agents to facilitate surface properties at relatively stable temperatures [13,14]. The pyrolysis

mechanism of the biomass material at lower temperatures as primary carbonized process is found to be beneficial in breaking palm leaves' microstructure and or chemical bonds, causing them to release gasses, tar and char [8]. In addition, pyrolysis mechanism at low temperature is also beneficial to convert the biomass materials into a fine grain powder by milling process to produce self-adhesive carbon grain [15-17].

The use of KOH for the activation of the biomass materials to prepare activated carbons with high surface area and porous sizes has been known [14-21]. It has been found that date palm leaves chemically activated with KOH synthesis active carbon with micropores and mesopores structure [14]. In addition it has been found that activated carbon based bituminous coal activated with KOH exhibits a high surface area of 3300 m^2/g [18].

Analysis of activated carbon can be made in terms of crystalline structure crystallite parameters (interlayer spacing (d_{002}) stack diameter (L_a) and stack height (L_c) amorphous content and strain, that are randomly distributed and oriented throughout the sample are very common [22-26]. It has been found that the crystallite parameters of the carbon material increased with the crystalline of the precursor [27] while the small crystallite perimeters reflected structure or defect as a resultant of higher porosity content [3]. Several attempted methods that have been used to improve the crystallite parameters, such as compression pressure [16,17] and increasing carbonization temperature or annealing process [28,29].

In different approaches, several researchers [30-34] identify two types of broadening; the crystal size and strain and the effects of simplified dislocation configurations on diffraction-line broadening were modeled. a) Dislocation model based on the mean square strain of dislocated crystals [33] and b)

A phenomenological model based on anisotropy of the elastic properties of crystals [35]. In addition, the size-broadened and strain-broadened profiles can be approximated by either the Voigt function (a convolution of the Lorentz and Gaussian function) or the Double Voigt function [36]. So far, many theories and methods have been used to estimate the crystallite parameters (Debye-Scherrer equation), line-broadening analysis and strain broadening [18-32] and amorphous content [25,26].

In the present research, the biomass date palm leaves were used as stating material for preparation of activated carbon by chemical activation with KOH. The crystallite parameters, amorphous contents and the functional groups of activated carbon activated by KOH were studied and compared with the review data. An X-ray diffraction trace program was used to calculate the crystallite dimensions to assess the accuracy.

Materials and Methods

Sample preparation

Initially date palm leaves were washed thoroughly to remove dust and other contamination and dried at 100°C. Then held in a box furnace (MPA6/400°C) equipped with a vacuum pump (Eyela, A-35), primary for pre-carbonized at 300°C for four causewayed a considerable weight loss with an average of 34% present. The pre-carbonized palm leaves were cut it to a small size and converted into a fine grain powder in a micro-hammer cutter for 20 hours a milling time to produce the self-adhesive properties. The grain power produced is stored in a clean, self-sealing plastic bag in silica gel until used. About 250 g powders were impregnated in a 1000 ml KOH solution having concentrations of 0.01, 0.02, 0.03, 0.04, 0.05, 0.06, 0.07 and 0.09 by moles (M). The mixture was magnetically stirred for one hour until mixed and kept for 16 h before being dried in an oven at 100°C for 24 h. The dried mixture was ball milled again for 5 hours and converted into a grain pellet (GPs) by applying 12 metric tons of pressure on 2 g of powder in a mold of 2.7 cm diameter and 8 cm length. The carbonization process was performed using the Vulcan Box Furnace (3-1750) at 1000°C in a nitrogen atmosphere in a heating chamber, starting at 1°C/min from room temperature to 375°C where it was held for 1 hour before heating was resumed at 3°C/min to 800°C and then 5°C/min to 1000°C which it was finally held for 5 minutes. Then the system was automatically allowed to cool down naturally to room temperature. Then samples were washed thoroughly by hot distilled water to clean their surface until a pH of 5 and then dried in an oven at 100°C for 4 hours. The diameter and thickness of the pellets were measured using a micrometer with six readings taken for each measurement and the average obtained. The bulk densities are determined by dividing their weight into volume.

X-ray diffractions

A series of measurements was carried out to characterize the structure of activated carbon samples by using X-ray diffraction techniques (Bruker Advanced Solution AXS D8) operating at 40 KV and 30 mA, with Cu Ka X-ray of wavelength (1.5404 Å). The measurements of X-ray diffraction were taken for each sample, at diffraction angle of 2⊖ over ranges of 7°C– 60°C, in steps size of 0.04°C as shown in Figure 1. Then diffraction intensity profiles recorded were corrected to the background line and instrumental broadening and then fitted into a symmetrical Gaussian distribution curve to release overlapping. The crystallite units of the carbon sample (d_{002}, L_c and L_a) can be calculated from the full width at half maximum (FWHM) of the (002), (100) and (110) diffraction peaks using Bragg's equation and Deby-Sherrier equation (Equation 1) displayed in Figure 2. An X-ray diffraction program (Trace 1.4) program from Diffraction Technology PTG LTD, Australia) refines the intensity of each peak (as a separate variable), the peak shape, as well as subtracts the background line and eliminates the Ka2-peak from the diffraction intensity that was used to calculate the crystallite parameters as shown in Figure 3.

$$L_{c,a} = \frac{K\lambda}{\beta \cos\theta} \tag{1}$$

Where K is the shape factor which is equal to 0.94 for L_c and 1.84 for L_a and β is the width of a reflection at half-maximum expressed in radians (Figures 1-3).

Amorphous content

According to the Debye-Scherrer equation the diffracted intensity $I(s)$, profiles comprised of three the components: (A) profile related to the crystalline size of the sample, $f(s)$, broadened by convolution with the profile due to instilment effects, $g(s)$ and the background line (BCL) [25,28] given as:

$$I(s) = f(s) x g(s) + BCL \tag{2}$$

Normalize diffraction intensity profiles by divided equation (2) by BCL as [37]

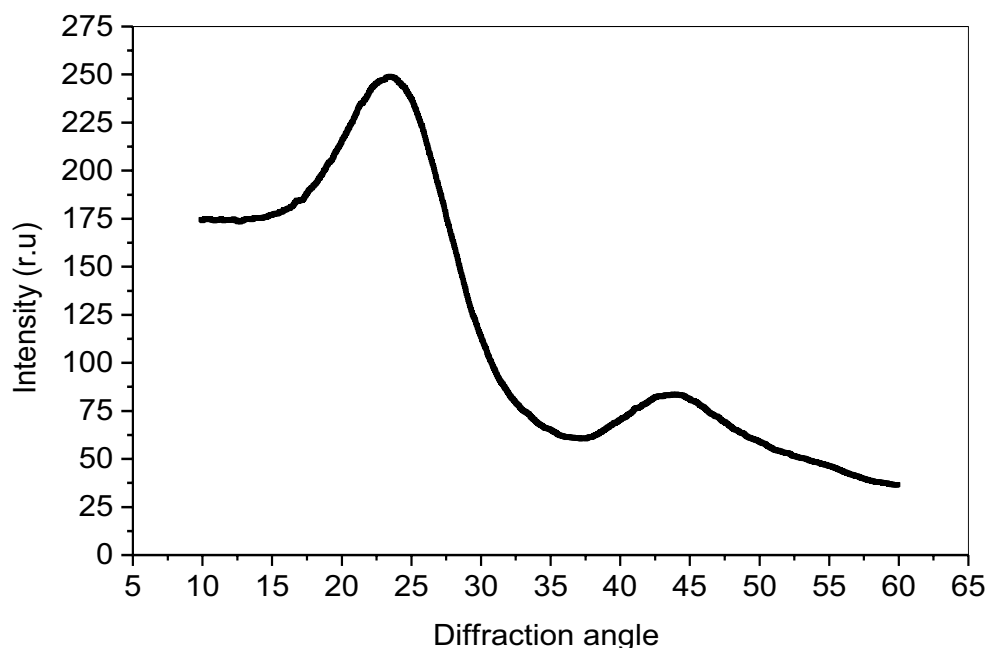$$1 = \frac{I(s)}{BCL} - \frac{f(s) x g(s)}{BCL} \tag{3}$$

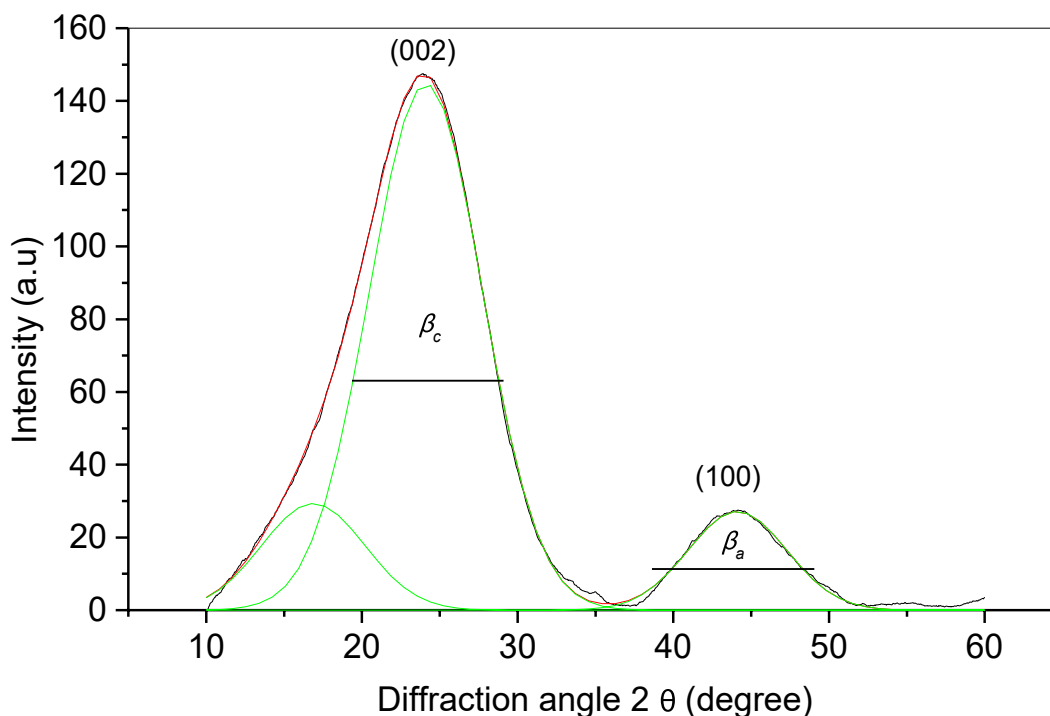**Figure 1.** X-ray diffraction of AC carbonized at 1000°C.

Figure 2. X-ray diffraction of AC corrected to a background line and fitted into Gaussian distribution curve.

The Deby-Scherrer interference equation rearranged in the atomic unit's as [25,26].

$$I(s) = \frac{1}{\sum f_p^2(s)} \sum \sum f^2(s)\left(\frac{\sin 2\pi sr}{2\pi sr}\right) \quad (4)$$

Where

$$s = \frac{2\pi \sin \theta}{\lambda}$$

f_p = is the scattering factor representing the background line

r = is the inter atomic distance

This involved two steps: (a) draw the background line within the total intensity oscillations (b) divide the total intensity by the background line to give an unsymmetrical reduced intensity J(s) in atomic units at the (002) peak [25]. Based on equation 2.11, the contribution from the amorphous content of the carbon pellets can be deducted from the scattering intensity in atomic units as given in Equation 2.13.

$$\left(\frac{(J(s)-xa)s^2}{0.0606(1-xa)}\right) = \sum_n P_n \left(\frac{\sin^2(n\pi d_{002}s)}{n\sin^2(\pi d_{002}s)}\right) = S_i(s)$$

Where,

x_a = is the fraction of amorphous structure given by the expression [25]

P_n = is the fraction of n layers associated in stacks having layered groups, $\sum_n P_n$ =1 and $S_i(s)$ = is a symmetrical reduced intensity.

The value of x_a first, plot $\left(\frac{(J(s)-x_a)s}{(1-x_a)0.0601}\right)$ vs. by selecting different values of x_a until a symmetrical curve is produced. Then, this symmetrical curve is fitted to equation 2.12 and the results obtained are used to adjust the value of x_a again, until both sides of the equation have been converted to the equivalent symmetrical form. Then the optimum value of x_a that which makes the profile the most symmetrical [25] (Figures 4 and 5).

FT-IR transmittance spectra

FT-IR Transmittance Spectra was carried out to analyze the functional groups of untreated and treated grain powder and activated carbon produced. FT selected ACP samples were crashed into powder and mixed with KBr and compacted to form thin pellets. The FTIR transmission spectra were collected using a RFX-65 spectrophotometer capable of a maximum resolution of 0.12 cm^{-1} and equipped with an MCT liquid nitrogen-cooled detector, interferometer, detector and computer software, (model-KVB/ Analects, INC). Infrared spectra were collected by using 2 to 5 milligrams (mg) of sample in a potassium bromide (KBr) pellet. The measurement was carried out using the Perkin Elmer System 2000 Fourier Transform Infrared (FTIR) with a pulsed laser carrier and a deutera-tedtriglycine sulfate detector. All the CPs was scanned from 400 to 4000 (cm^{-1}) averaging 10 scans at 1.0 cm^{-1} interval with a resolution of 0.25 cm^{-1}.

Results and Discussion

X-ray diffraction (XRD)

Figure 4 shows the X-ray diffraction profile diffraction intensity, initially at (002) and (100) broad and overlapped (002) and (100) reflection intensity results of non-graphic structure [24]. Similar observations have been shown for activated carbon-based petroleum [2] and solid carbon pellets from date palm leaves prepared at different compression pressures [16]. The diffraction profile has been corrected to the background line and fitted to the Gaussian distribution curve as shown. As the diffraction profile overlaps and consists of four broad intensity peaks i.e. (002), (100) and (004) corresponding diffraction angles are 25.36°C, 45.1°C and 52.85°C diffraction angles, respectively. After correction, the diffraction intensity and Bragg's peaks were the same as in a graphite-like structure and the layer separation was slightly further apart than in a graphite structure as shown in Figure 4.

Figure 5 show that the interlayer spacing (d_{002}) increased linearly with increasing the KOH concentration, indicating that the carbon samples had a high degree of disorientation or slightly non-graphitic structure [38]. The results can be interpreted as: the KOH first reacts with the surface functional groups in grain powder and then some carboxyl and/or its compounds intercalate by reducing the crystalline layers of the activated carbon produced to Figure 6 showing the crystallite parameters (L_c and L_a) of the AC decreased continually with increasing KOH treatment. A decrease in the crystallite parameters of the CPs may lead to the development of the pore structure in the carbon sample produced compared to the AC prepared from
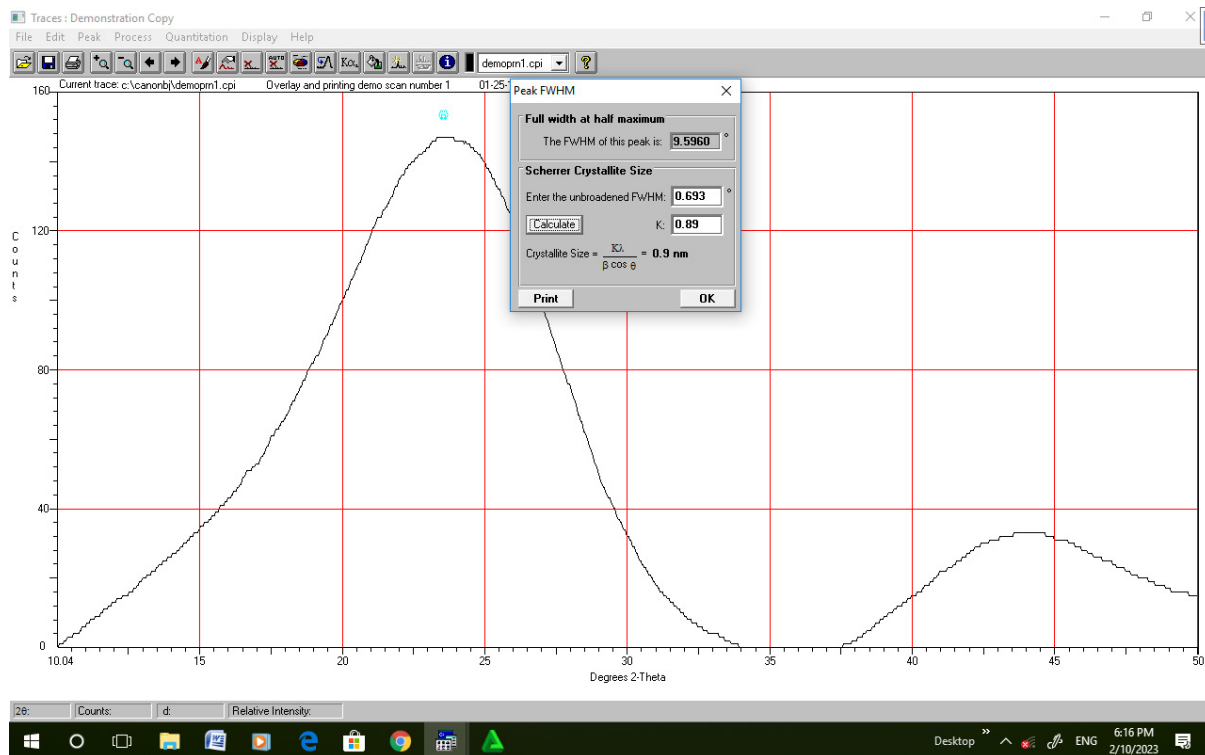
Figure 3. Trace X-ray diffraction program used to determine crystallite parameters.
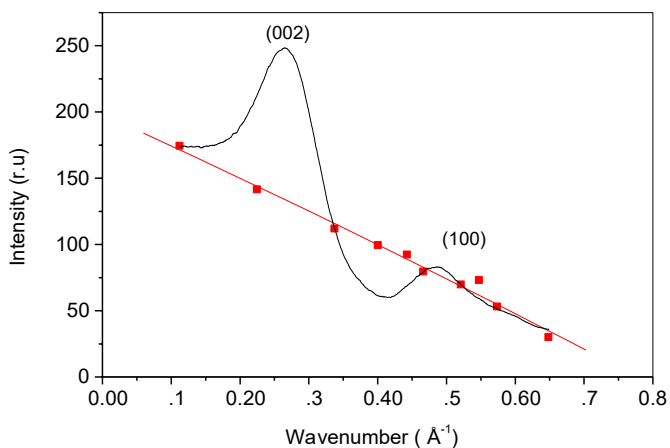

Figure 4. X-ray diffraction intensity of AC corrected for background line within layer.
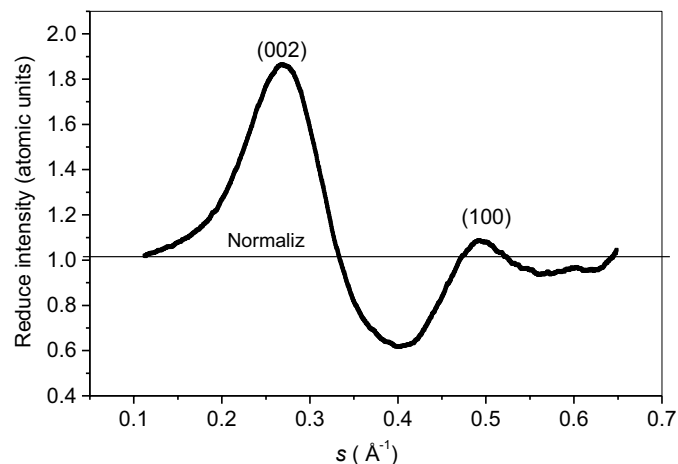

Figure 5. X-ray diffraction intensity of AC normalized into reduces intensity.

untreated and that treatment with different concentration of KOH. A similar result on crystallite parameters was observed on solid carbon pellets from date palm leaves prepared by using different compression pressure [16]. The data of d_{002}, L_c and L_a were compared to those of AC prepared from olive stones [38-41] coal tar pitch (CTP) carbonized at 800°C and commercial AC (AC-Helas) were found to be in good agreement, but L_a is larger than that of commercial AC [24] (Figures 6 and 7).

Amorphous content

The asymmetry reduced the intensity of $J(s)$ from the X-ray diffraction, so that the value of the amorphous fraction (x_a) was adjusted for the plot of Si (s) vs. s to become symmetrical as shown in Figure 8. Indicating that it is possible to obtain a very precise fit by testing a considerable number of n distributions at the (002) peak of reduced intensity in atomic units for the AC sample treated by 0.07 M KOH [25]. The expression used to estimate the amorphous fraction is very sensitive to the proper choice of x_a, whose optimum value is that which makes the reduced intensity Si (s) at (002) Bragg's peak, most symmetrical. Also, Figure 8 illustrates the effects on the Si (s) profile of using different values of n until match. Figure 9 shows the good
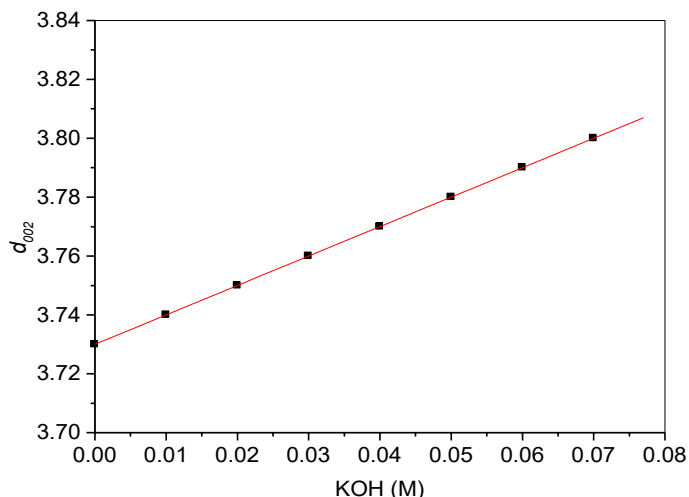

Figure 6. d_{002} vs. KOH.

agreement obtained by matching the value of n to the experimental values of the reduced intensity profiles Si (s). The symmetrical profile measurements give the value x_a of 0.59, for the AC treated with 0.07 M KOH, indicating the structure of the carbon sample to be about 59 percent amorphous. The adjusted fitted curve gives Pn = 0.0359, n = 3, S*max = 0.2612 Å^{-1}. The values of x_a decreased and increased greatly as the KOH concentration increased from 0 to 0.07 M. These findings indicate that the KOH applied on palm leaves grain powder can transform the activated carbon structure into a more amorphous state (Table 1, Figures 8 and 9).

FT-IR transmittance of activated carbon (AC)

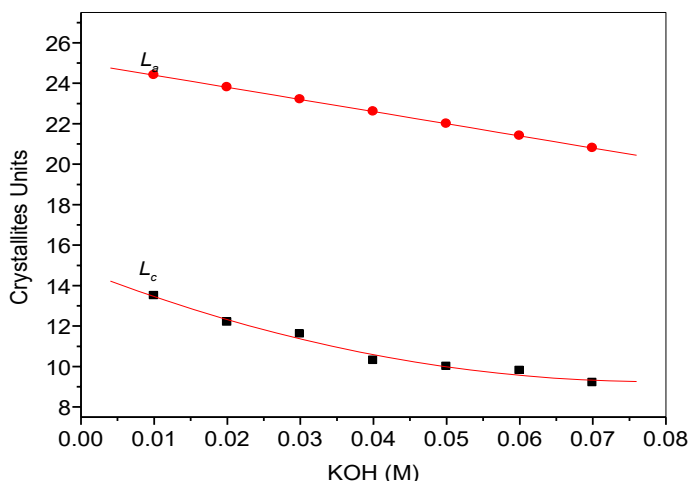FTIR transmission spectra of the AC show broad bands were observed

Figure 7. L_a and L_c *vs.* KOH.

Table 1. Represent amorphous contents of the activated carbon pellets as a function of KOH concentrations by moles.

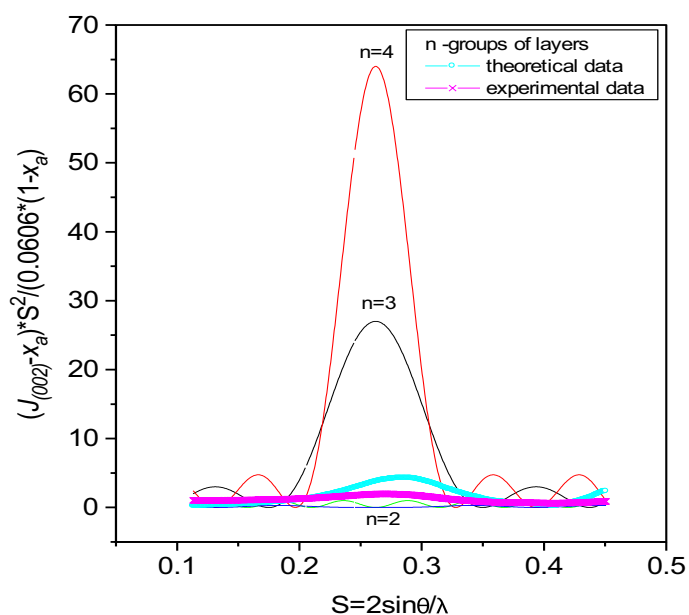| KOH (M)	Xa %
0.00	50
0.01	49
0.02	48
0.03	51
0.04	54
0.05	56
0.06	57
0.07	59

Figure 8. X-ray diffraction intensity of AC corrected for background line within layer.
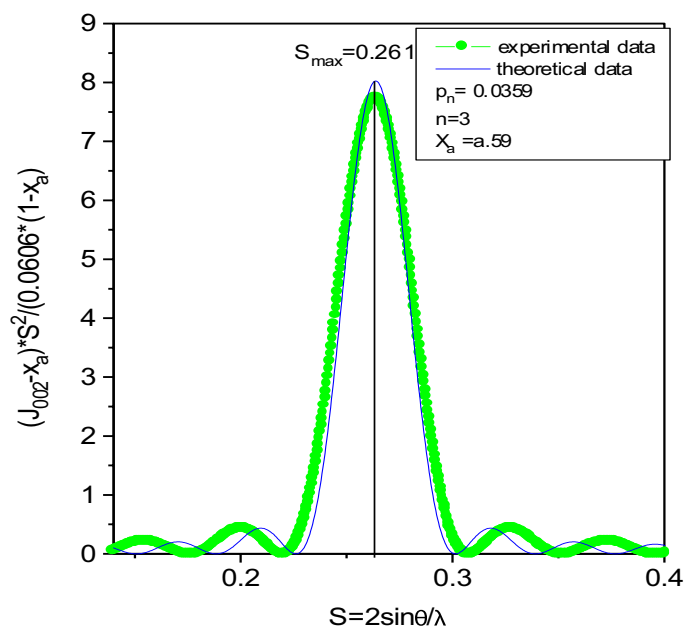

Figure 9. X-ray diffraction intensity of AC corrected for background line within layer.
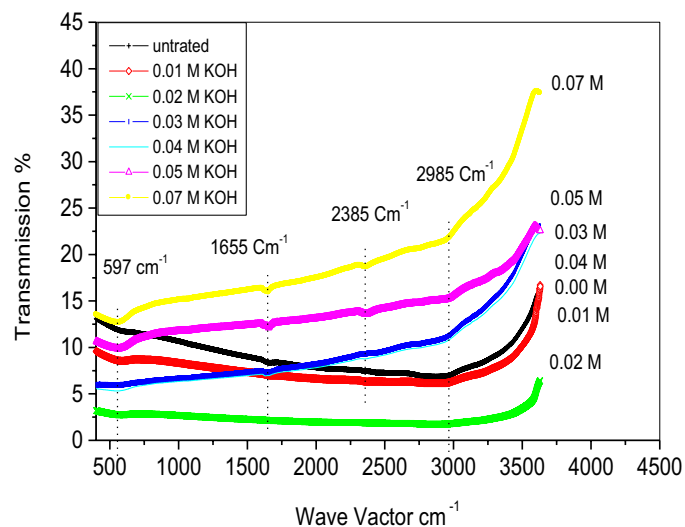

Figure 10. FTIR data for the untreated and treated grain powder with KOH.

in all untreated and treated grain powder samples. The adsorption is at 597 cm^{-1}, which can be assigned to C-H stretching vibrations in the carbonyl groups and at 1069 cm^{-1} due to C-O-C stretching [42]. The band at 1652 cm^{-1} was due to C=O stretching in the aromatic rings. The FTIR spectrum showed a band at 2365 cm^{-1} due to C=C, probably from the alkaline groups and a band at 2939 cm^{-1} due to asymmetric C–H stretching vibrations, indicating the presence of some aliphatic species, such as olefins or acetylene groups (Figure 10).

Conclusion

X-ray diffraction profiles show that the structure of activated carbon produced is non-graphitic. The interlayer spacing (d_{002}) increased linearly with increasing KOH concentrations, while stack diameter (L_a) and stack height (L_c) of the graphitic like crystal were observed to decrease with increasing KOH concentrations. The amorphous contents increased with KOH concentration.

The FTIR transmission spectrum shows a broad absorbing band for the carbon pellets and showed that C=C stretching vibration. The data also, the FTIR transmission spectrum of the carbon pellets carbonized at 1000°C

showed the presence of some absorption bands that are related to organic compounds, which were still not completely released in the AC pellets at this temperature.

Acknowledgements

Conflict of Interests

None.

References

1. Berrios, Monica, Maria Angeles Martin and Antonio Martin. "Treatment of pollutants in wastewater: Adsorption of methylene blue onto olive-based activated carbon." *J Ind Eng Chem* 18 (2012): 780-784.

2. Ahmed, Muthanna J. "Preparation of activated carbons from date (*Phoenix dactylifera* L.) Palm stones and application for wastewater treatments." *Process Saf Environ Prot* 102 (2016): 168-182.

3. Benedetti, Vittoria, Francesco Patuzzi and Marco Baratieri. "Characterization of char from biomass gasification and its similarities with activated carbon in adsorption applications." *Appl Energy* 227 (2018): 92-99.

4. Yue, Jing, Jiaqi Yu, Shaohua Jiang and Yiming Chen. "Biomass carbon materials with porous array structures derived from soybean dregs for effective electromagnetic wave absorption." *Diam Relat Mater* 126 (2022): 109054.

5. Rawat, Shivam, Rakesh K. Mishra and Thallada Bhaskar. "Biomass derived functional carbon materials for supercapacitor applications." *Chemosphere* 286 (2022): 131961.

6. Arof, Abdul Kariem, M. Z. Kufian, M. F. Syukur and M. F. Aziz, et al. "Electical double layer capacitor using poly (Methyl methacrylate)-C4BOLi gel polymer electrolyte and carbonaceous material from Shells of mata Kucing (*Dimocarpus Longan*) fruit." *Electrochimica Acta* 74 (2012): 39-45.

7. Köseoğlu, Eda and Canan Akmil-Başar. "Preparation, structural evaluation and adsorptive properties of activated carbon from agricultural waste biomass." *Adv Powder Technol* 26 (2015): 811-818.

8. Dhyani, Vaibhav and Thallada Bhaskar. "A comprehensive review on the pyrolysis of lignocellulosic biomass." *Renew Energy* 129 (2018): 695-716.

9. González-García, P. "Activated carbon from lignocellulosics precursors: A review of the synthesis methods, characterization techniques and applications." *Renewable Sustainable Energy Rev* 82 (2018): 1393-1414.

10. Fermanelli, Carla S., Agostina Córdoba, Liliana B. Pierella and Clara Saux. "Pyrolysis and copyrolysis of three lignocellulosic biomass residues from the agro-food industry: A comparative study." *J Waste Manag.* 102 (2020): 362-370.

11. Chanpee, Sirayu, Napat Kaewtrakulchai, Narathon Khemasiri and Apiluck Eiad-Ua, et al. "Nanoporous carbon from oil palm leaves *via* hydrothermal carbonization-combined KOH activation for paraquat removal." *Molecules* 27 (2022): 5309.

12. Yi, Hyeonseok, Koji Nakabayashi, Seong-Ho Yoon and Jin Miyawaki. "Pressurized physical activation: A simple production method for activated carbon with a highly developed pore structure." *Carbon* 183 (2021): 735-742.

13. El-Sayed, Gamal O., Mohamed M. Yehia and Amany A. Asaad. "Assessment of activated carbon prepared from corncob by chemical activation with phosphoric acid." *Water Resour Ind* 7 (2014): 66-75.

14. Fatima M. A., Zehhba A. A., Rehab O. E. and Abubaker E. A, et al. "Characterization of pores size, surface area and fractal dimensions of activated carbon powder prepared from date palm leaves." *Mol Bio* 11 (2022b): 352.

15. Taer, Erman, Nazilah Nikmatun, Rika Taslim and Ezri Hidayat. "The self-adhesive carbon powder based on coconut coir fiber as supercapacitor application." *J Metastab Nanocryst Mater* 33 (2021): 1-11.

16. Abdelrahman, Abubaker Elsheikh and Co-Author Dr Selma Elsheikh Abdelrahman. "Crystallites dimensions and electrical conductivity of Solid Carbon Pellets (SCPs) from date palm leaves (*Phoenix dactylifera* L.)." *Acad J Res Sci Pub* 4 (2023).

17. Hsu, Li-Yeh and Hsisheng Teng. "Influence of different chemical reagents on the preparation of activated carbons from bituminous coal." *Fuel Process Technol* 64 (2000): 155-166.

18. Okman, Irem, Selhan Karagöz, Turgay Tay and Murat Erdem. "Activated carbons from grape seeds by chemical activation with potassium carbonate and potassium hydroxide." *Appl Surf Sci* 293 (2014): 138-142.

19. Pagketanang, Thanchanok, Apichart Artnaseaw, Prasong Wongwicha and Mallika Thabuot. "Microporous activated carbon from KOH-activation of rubber seed-shells for application in capacitor electrode." *Energy Procedia* 79 (2015): 651-656.

20. Yang, H. M., D. H. Zhang, Y. Chen and M. J. Ran, et al. "Study on the application of KOH to produce activated carbon to realize the utilization of distiller's grains." *IOP Conf Ser Earth Environ Sci* 69 (2017): 012051.

21. Deraman, Mohamad, Sarani Zakaria and Julie Andrianny Murshidi. "Estimation of crystallinity and crystallite size of cellulose in benzylated fibres of oil palm empty fruit bunches by X-ray diffraction." *Jpn J Appl Phys* 40 (2001): 3311.

22. Song, Dangyu, Cunbei Yang, Xiaokui Zhang and Xianbo Su, et al. "Structure of the organic crystallite unit in coal as determined by X-ray diffraction." *Min Sci Technol (China)* 21 (2011): 667-671.

23. Faber, Kristin, Felix Badaczewski, Wilhelm Ruland and Bernd M. Smarsly. "Investigation of the microstructure of disordered, non-graphitic carbons by an advanced analysis method for wide-angle x-ray scattering." *Z fur Anorg Allg Chem* 640 (2014): 3107-3117.

24. Lu, Liming, V. Sahajwalla, C. Kong and D. Harris. "Quantitative X-ray diffraction analysis and its application to various coals." *Carbon* 39 (2001): 1821-1833.

25. Ergun, Sabri. "Analysis of coherence, strain, thermal vibration and preferred orientation in carbons by X-Ray diffraction." *Carbon* 14 (1976): 139-150.

26. Kim, Dae-Young, Yoshiharu Nishiyama, Masahisa Wada and Shigenori Kuga. "Graphitization of highly crystalline cellulose." *Carbon* 39 (2001): 1051-1056.

27. Suzuki, T. and K. Kaneko. "The micrographite growth of activated carbon fibers with high temperature treatment studied by computer-aided X-ray diffraction." *Carbon* 31 (1993): 1360-1361.

28. Emmerich, F. G. and C. A. Luengo. "Young's modulus of heat-treated carbons: A theory for nongraphitizing carbons." *Carbon* 31 (1993): 333-339.

29. Langford, J. Il. "A rapid method for analysing the breadths of diffraction and spectral lines using the Voigt function." *J Appl Crystallogr* 11 (1978): 10-14.

30. Rietveld, Hugo M. "A profile refinement method for nuclear and magnetic structures." *J Appl Crystallogr* 2 (1969): 65-71.

31. Iwashita, Norio and Michio Inagaki. "Relations between structural parameters obtained by X-ray powder diffraction of various carbon materials." *Carbon* 31 (1993): 1107-1113.

32. Ungár, Tamás, Jenő Gubicza, Gábor Ribárik and A. Borbély. "Crystallite size distribution and dislocation structure determined by diffraction profile analysis: Principles and practical application to cubic and hexagonal crystals." *J Appl Crystallogr* 34 (2001): 298-310.

33. Ungár, T. and A. Borbély. "The effect of dislocation contrast on x-ray line broadening: A new approach to line profile analysis." *Appl Phys Lett* 69 (1996): 3173-3175.

34. Stephens, Peter W. "Phenomenological model of anisotropic peak broadening in powder diffraction." *J Appl Crystallogr* 32 (1999): 281-289.

35. Sánchez-Bajo, Florentino, Angel L. Ortiz and Francisco L. Cumbrera. "Analytical formulation of the variance method of line-broadening analysis for Voigtian X-ray diffraction peaks." *J Appl Crystallogr* 39 (2006): 598-600.

36. Abubaker, E.A., "Physical and electrical properties of carbon pellets from cotton cellulose." *Thesis* (2006).

37. Yakout, S. M. and G. Sharaf El-Deen. "Characterization of activated carbon prepared by phosphoric acid activation of olive stones." *Arab J Chem* 9 (2016): S1155-S1162.

38. Zuo, Songlin, Jianxiao Yang, Junli Liu and Xuan Cai. "Significance of the carbonization of volatile pyrolytic products on the properties of activated carbons from phosphoric acid activation of lignocellulosic material." *Fuel Process Technol* 90 (2009): 994-1001.

39. Zhang, Su, Jin Niu, Huaihe Song and Lingxiang Zhu, et al. "Can closed shell graphitic materials be exfoliated? Defect induced porphyra-like graphene from the cooperation of activation and oxidation." *J Mater Chem A* 1 (2013): 14103-14107.

40. Zhang, Dengfeng, Shilin Liu, Xuexiang Fu and Shuaiqiu Jia, et al. "Adsorption and desorption behaviors of nitrous oxide on various rank coals: Implications for oxy-coal combustion flue gas sequestration in deep coal seams." *Energy Fuels* 33 (2019): 11494-11506.

41. Acik, Muge, Geunsik Lee, Cecilia Mattevi and Adam Pirkle, et al. "The role of oxygen during thermal reduction of graphene oxide studied by infrared absorption spectroscopy." *J Phys Chem C* 115 (2011): 19761-19781.

42. Horikawa, Toshihide, Yoshiyuki Kitakaze, Tomoki Sekida and Jun'ichi Hayashi, et al. "Characteristics and humidity control capacity of activated carbon from bamboo." *Bioresour Technol* 101 (2010): 3964-3969.